# Supporting Information

## High contrast NIR excitation probe monitoring $Cu^{2+}$ in the endoplasmic reticulum for synergistic cuproptosis and ferroptosis anticancer therapy

Jingjing Jiang[a], Qiong Zhang[a*], Yue Zhang[a], Lintong Gao[a], Yan Feng[a*], Xianshun Sun[a], Junjun Wang[a], Xingxing Chen[a], Hongping Zhou[a,b*]

[a] School of Chemistry and Chemical Engineering, Center of Free Electron Laser & High Magnetic Field, Key Laboratory of Structure and Functional Regulation of Hybrid Materials Ministry of Education, Key Laboratory of Functional Inorganic Materials Chemistry of Anhui Province, and Key Laboratory of Chemistry for Inorganic/Organic Hybrid Functionalized Materials of Anhui Province, Anhui University.
[b] School of Chemical and Environmental Engineering, Anhui Polytechnic University, 241000, Wuhu, P.R. China.
E-mail: zhangqiong.314@163.com, fy70@163.com, zhpzhp@263.net.

## Experimental methods

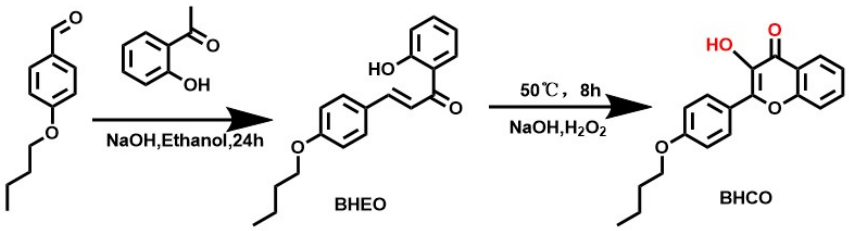


**Fig. S1** The synthesis route of BHCO.

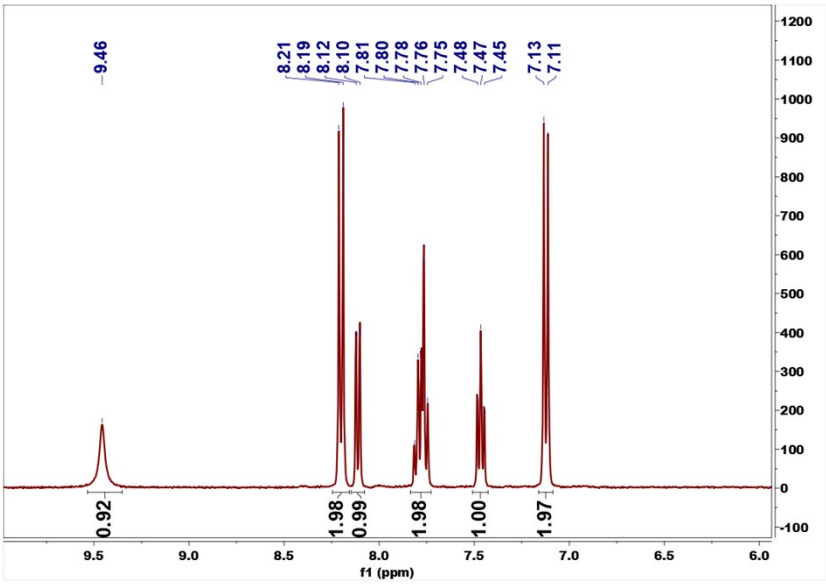


**Fig. S2** $^{1}$H NMR spectrum of BHCO.

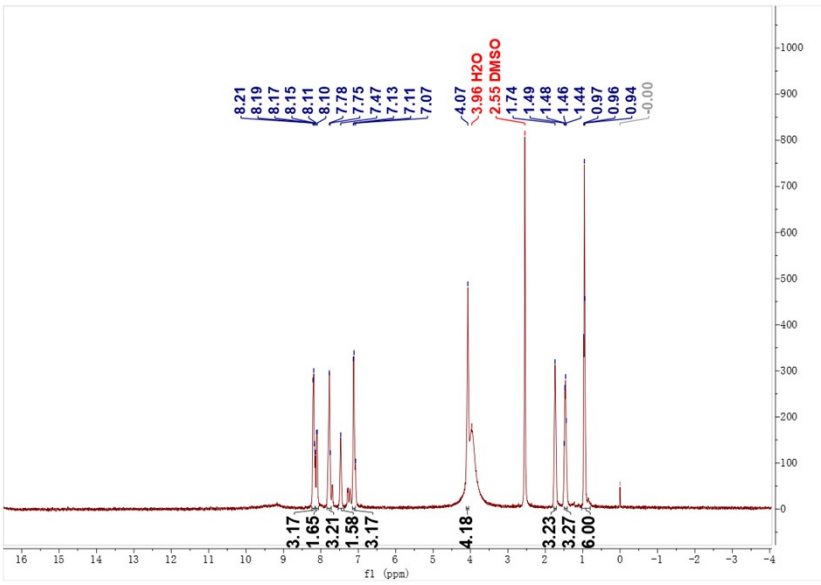


**Fig. S3** $^{1}$H NMR of Cu2BC.

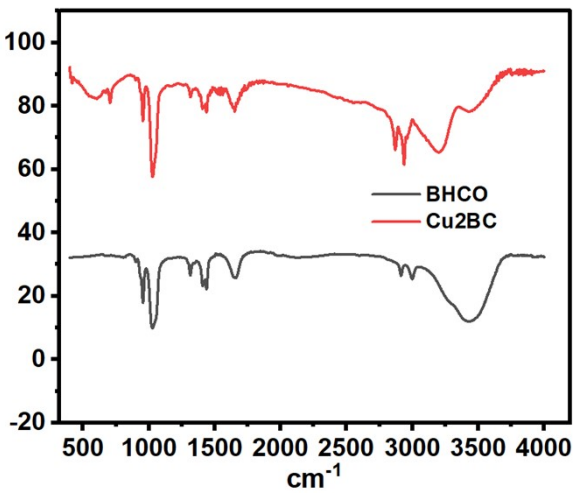


**Fig. S4** IR spectrometry validation of Cu2BC.

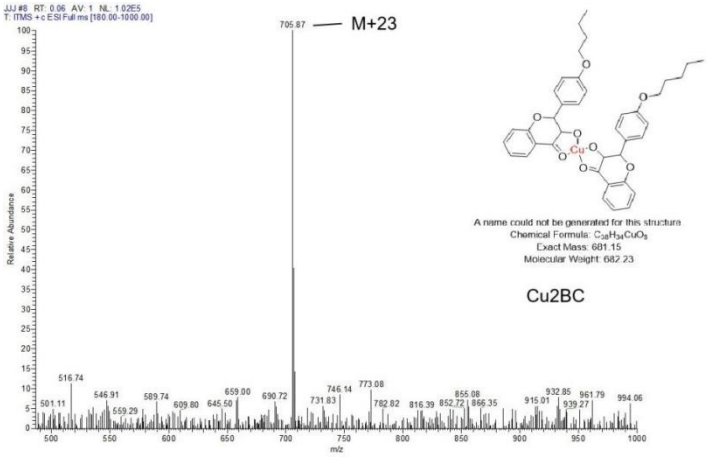


**Fig. S5** Mass spectrometry validation of Cu2BC.

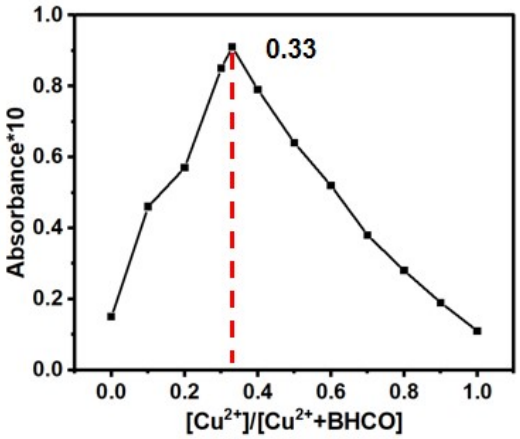


**Fig. S6** Job's plot analysis with various mole fractions of BHCO and $Cu^{2+}$.

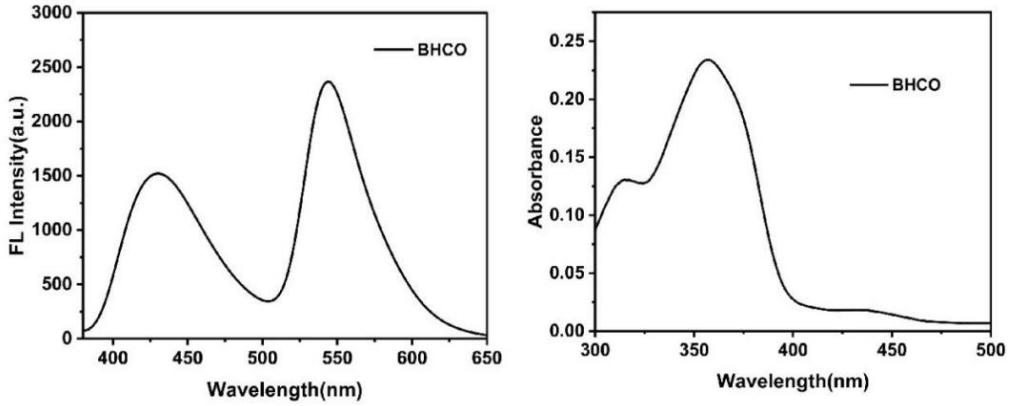


**Fig. S7** The fluorescence emission and UV-vis absorption spectra of BHCO.

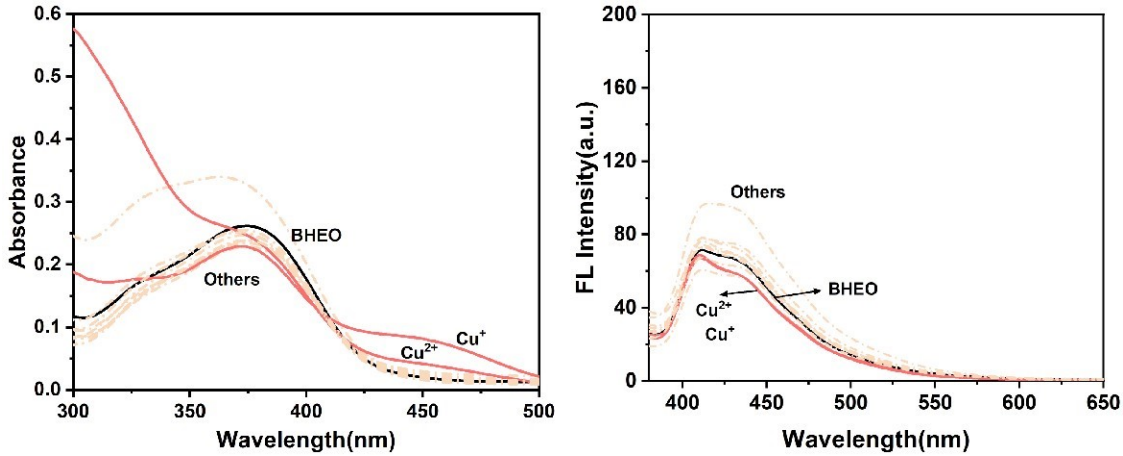


**Fig. S8** The UV-vis absorption and fluorescent spectra of BHEO (5.0 μM) with $Cu^{2+}$ and other analytes ($K^+$, $Ca^{2+}$, $Na^+$, $Fe^{3+}$, $Fe^{2+}$, $Mg^{2+}$, $Zn^{2+}$, $SO_4^{2-}$, $CO_3^{2-}$, $SO_3^{2-}$, $Cl^-$, GSH, Cys, Hcy =10.0 μM) in DMSO.

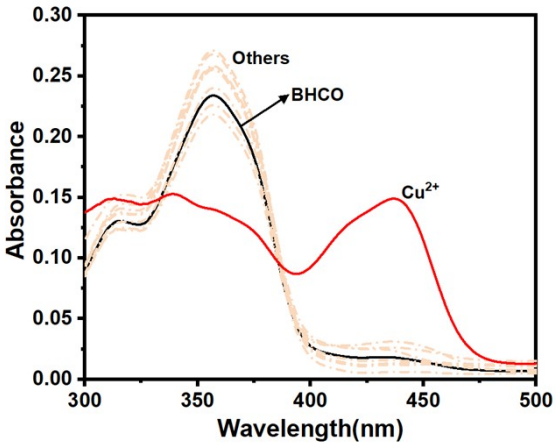


**Fig. S9** The UV-vis absorptionspectra of BHCO (5.0 μM) with $Cu^{2+}$ and other analytes ($K^+$, $Ca^{2+}$, $Na^+$, $Fe^{3+}$, $Fe^{2+}$, $Mg^{2+}$, $Zn^{2+}$, $SO_4^{2-}$, $CO_3^{2-}$, $SO_3^{2-}$, $Cl^-$, GSH, Cys, Hcy =10.0 μM) in DMSO.

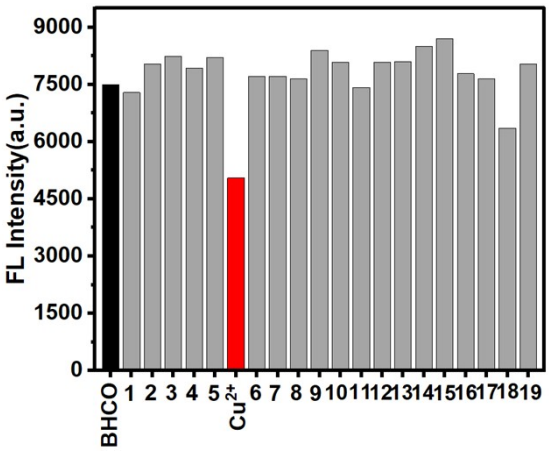


**Fig. S10 The competition experiment. Effect of the presence of other analytes on the recognition of $Cu^{2+}$ by BHCO.** 1-18: $K^+$, $Ca^{2+}$, $Na^+$, $Fe^{3+}$, $Fe^{2+}$, $Mg^{2+}$, $Zn^{2+}$, $SO_4^{2-}$, $CO_3^{2-}$, $SO_3^{2-}$, $Cl^-$, $ClO^-$, $H_2O_2$, $H_3PO_4^-$, Cholinesterase (Che), $NH_4^+$, Tyrosine (Tyr), Glucose (Glu), Serine (Ser), Cys, Hcy, GSH.

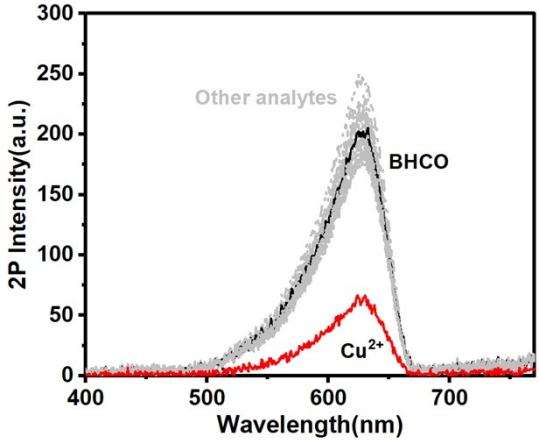


**Fig. S11** The two-photon fluorescence spectroscopy of BHCO (10 μL, 2mM) in the presence of various analytes. Others analytes: $K^+$, $Ca^{2+}$, $Na^+$, $Fe^{3+}$, $Fe^{2+}$, $Mg^{2+}$, $Zn^{2+}$, $SO_4^{2-}$, $CO_3^{2-}$, $SO_3^{2-}$, $Cl^-$, $ClO^-$, $H_2O_2$, $H_3PO_4^-$, Cholinesterase, $NH_4^+$, Tyrosine(Tyr), Glucose(Glu), Serine(Ser), Cys, Hcy, GSH (Ex=720 nm; Em=600 nm).

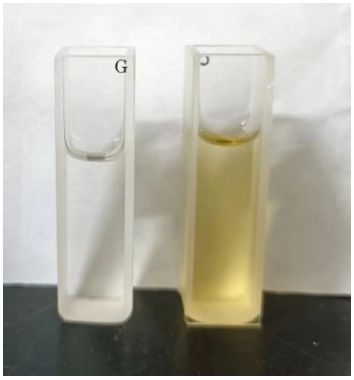


**Fig. S12** Color changes of DMSO solution before and after BHCO and $Cu^{2+}$ reaction.

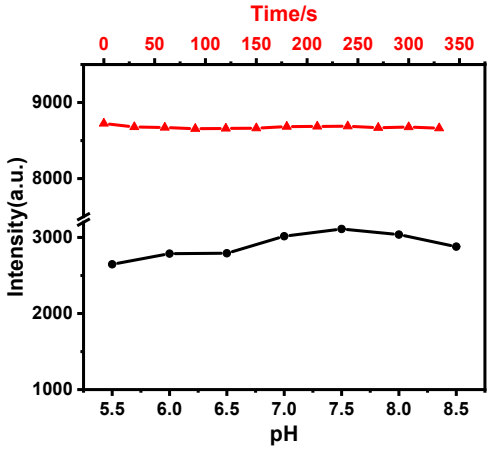


**Fig. S13** The time stability of BHCO before the reaction within 5 min and stability of fluorescence in different pH after the reaction (5.5-8.5).

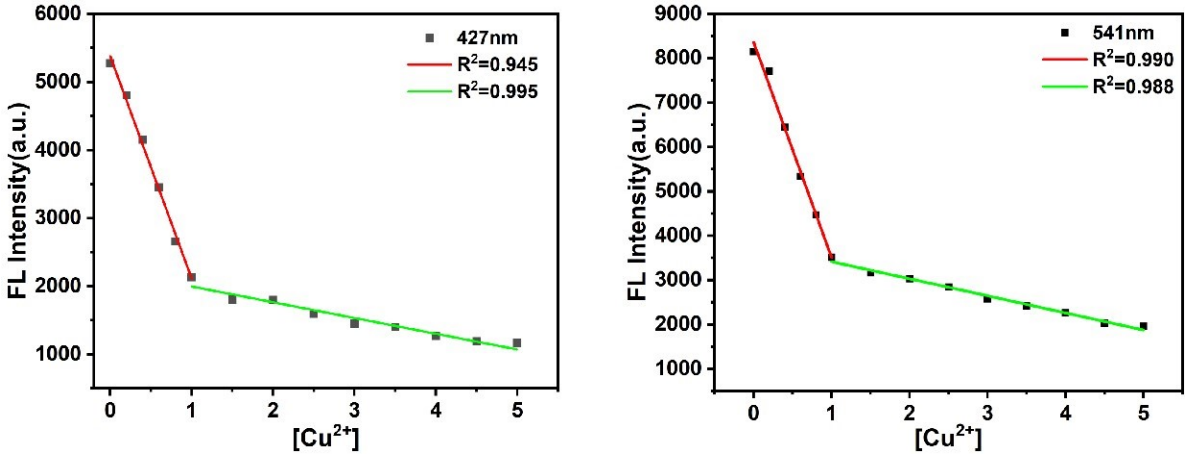


**Fig. S14** The linear fitting of fluorescent peak of BHCO (10 μL) at different concentrations of $Cu^{2+}$ (0-5 μL, 1 mM) at 427 nm and 541 nm.

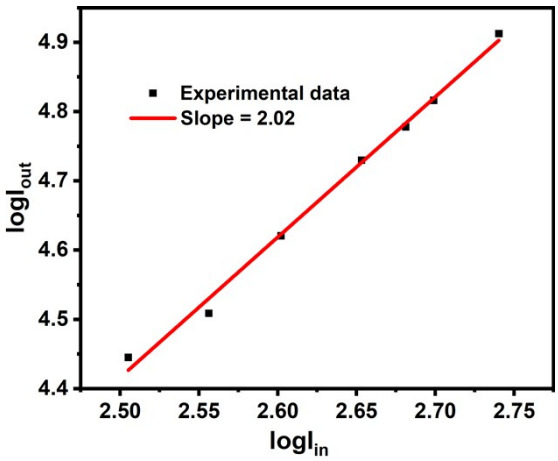


**Fig. S15** Two-photon absorption validation about BHCO.

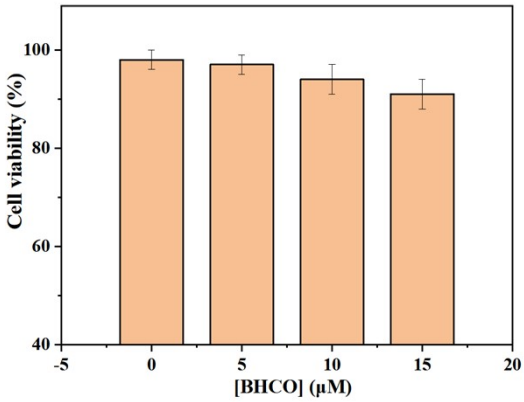


**Fig. S16** Cell viabilities of HeLa cells incubated with different concentrations of BHCO (0-15 μM).

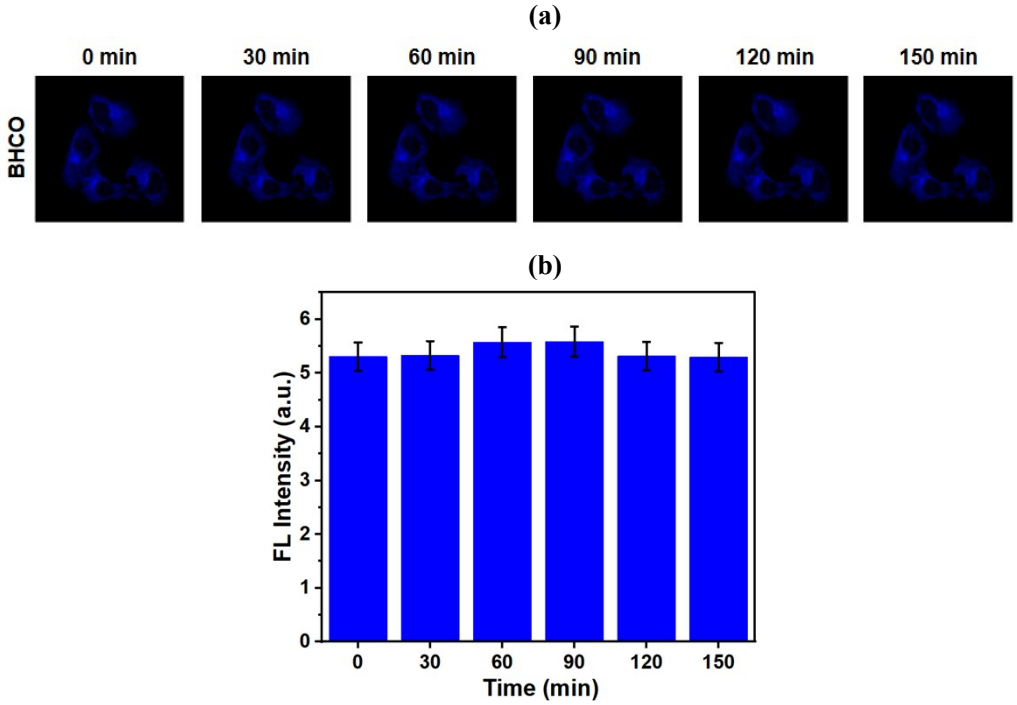


**Fig. S17** BHCO (5μM) staining of HeLa cells was observed fluorescence-imaging at various intervals (0 min, 30 min, 60 min, 90 min, 120 min, 150 min).

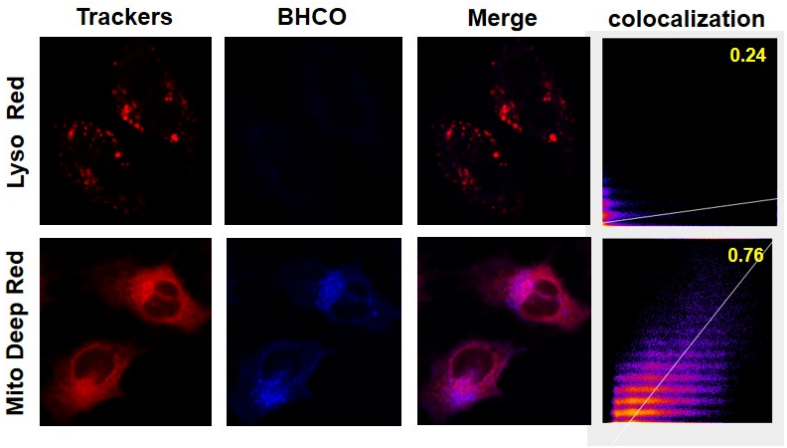


**Fig. S18** Co-localization experiment. Confocal images of the HeLa cells stained with BHCO

(10 μL) and Lyso Red (10 μL), Mito Deep Red (10 μL); fluorescence intensity correlation plot for BHCO and lysosomes and mitochondria, separately.

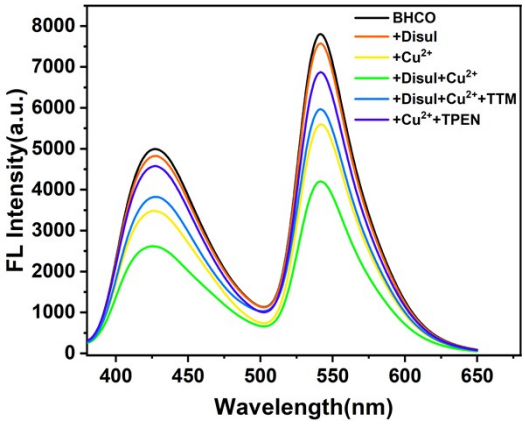


**Fig. S19** Fluorescence emission spectra of BHCO when different drugs are added.

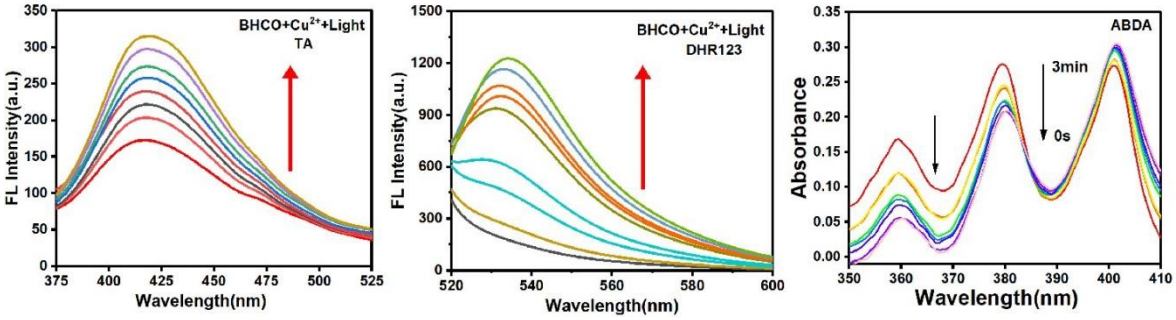


**Fig. S20** *In vitro* measurement of ROS production by BHCO (10 μM) and $Cu^{2+}$ (15 μM) in the presence or absence of light source.

Detection of OH· content based on fluorescence emission intensity at 435 nm when TA is excited at 315 nm; The content of $O_2^{\bullet-}$ was detected using DHR123 under excitation at 505 nm and emission at 535 nm; Detect the content of $^1O_2$ based on the decrease of ABDA's UV absorption peak at 378nm under light or no light conditions.

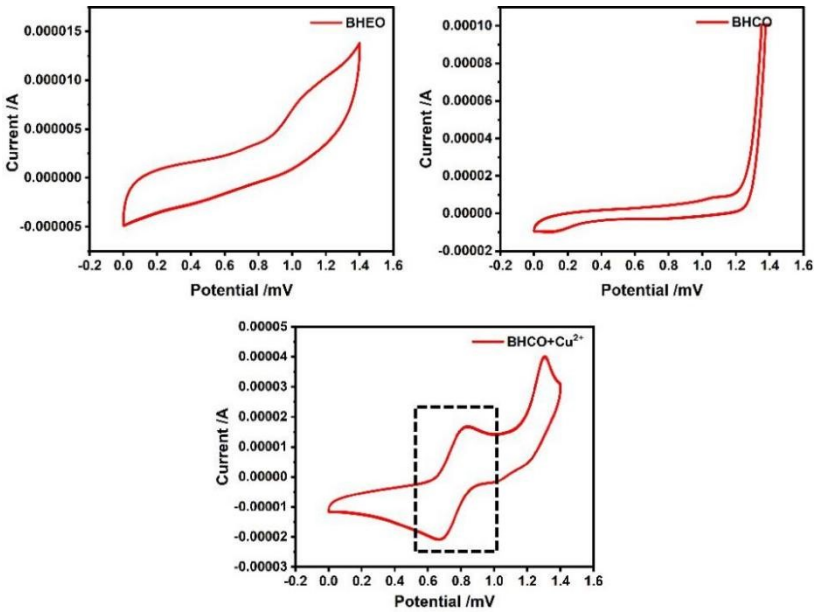


**Fig. S21** Cyclic-voltammetric (CV) of BHEO/BHCO/BHCO-$Cu^{2+}$ in $CH_3CN$. (c = $1\times10^{-5}$ mol/L, scan rate = 100 mV/s)

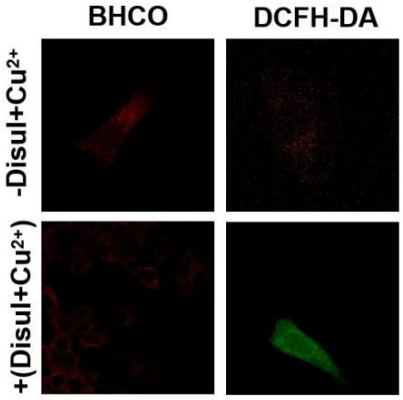


**Fig. S22** ROS imaging of HeLa cells pretreated with or without BHCO, DSF (50 μM) and $Cu^{2+}$. BHCO is used to image the total intracellular $Cu^{2+}$. DCFH-DA is used to image the total amount of intracellular ROS.

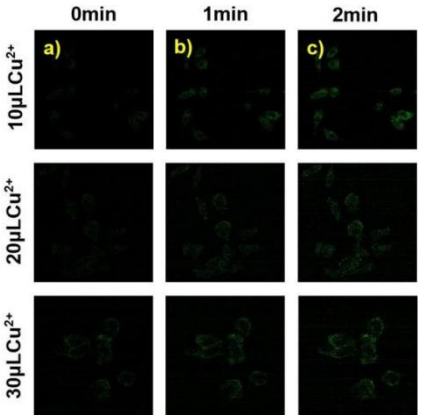


**Fig. S23** Effect of copper content and different durations of light on OH· production. (a-c) Measure the intracellular OH· content by HPF under the conditions of changing the

concentration of copper ions and light exposure time.

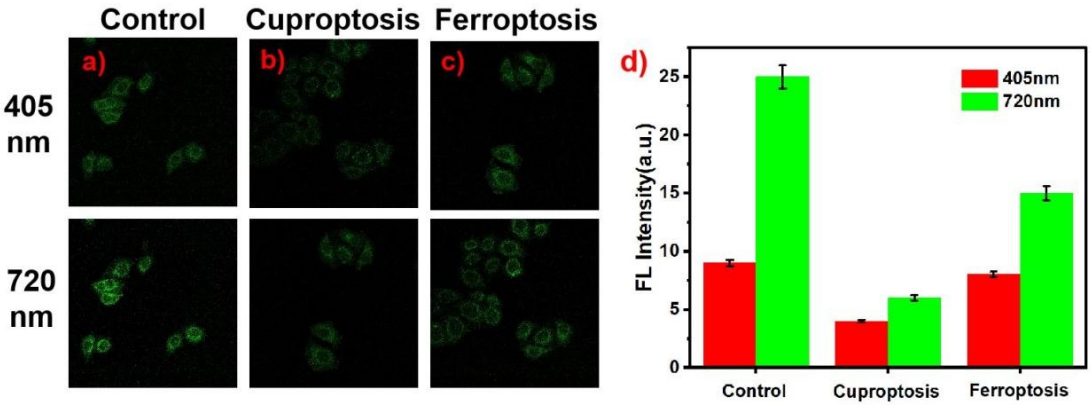


**Fig. S24** Effect of changing the wavelength on the ROS.
(a-c)The effect of adding ferroptosis inhibitor Fer-1 or cuproptosis inhibitor TTM at different wavelengths on the total intracellular ROS by DCFH-DA. (d) Bar charts of fluorescence intensity for different groups.

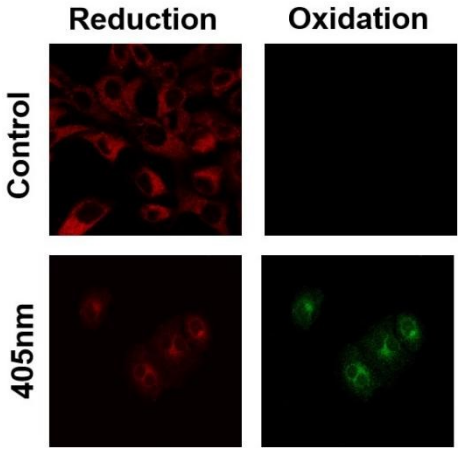


**Fig. S25** Lipid peroxidation process detection was induced by DSF and $Cu^{2+}$ and detected by C11-BODIPY 581/591.
The lipid peroxidation levels were measured in the untreated control group and light control group treated with single photon 405 nm laser respectively. Reduced state (red color): 581/591 nm. Oxidized state (green color): 488/510 nm.

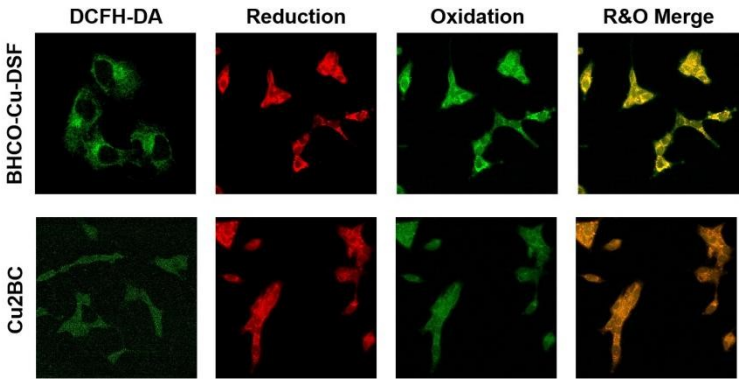


**Fig. S26** ROS and lipid peroxidation assays by Cu2BC and BHCO-Cu-DSF. Intracellular ROS by

DCFH-DA; Lipid peroxidation process detected by C11-BODIPY 581/591.

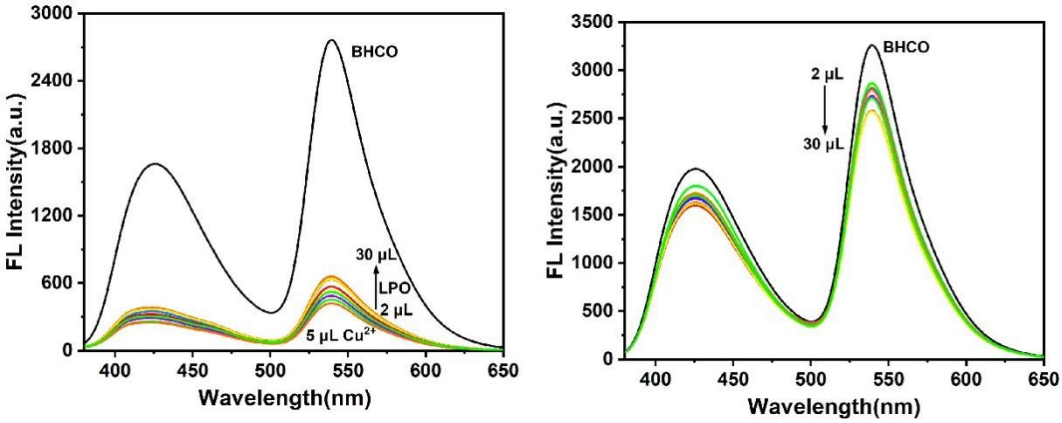


**Fig. S27** The fluorescence spectra of the BHCO (10 μL, 2 mM) with LPO (2-30 μL, 1 mM) in a) the absence and b) the presence of $Cu^{2+}$ (5 μL,1 mM).

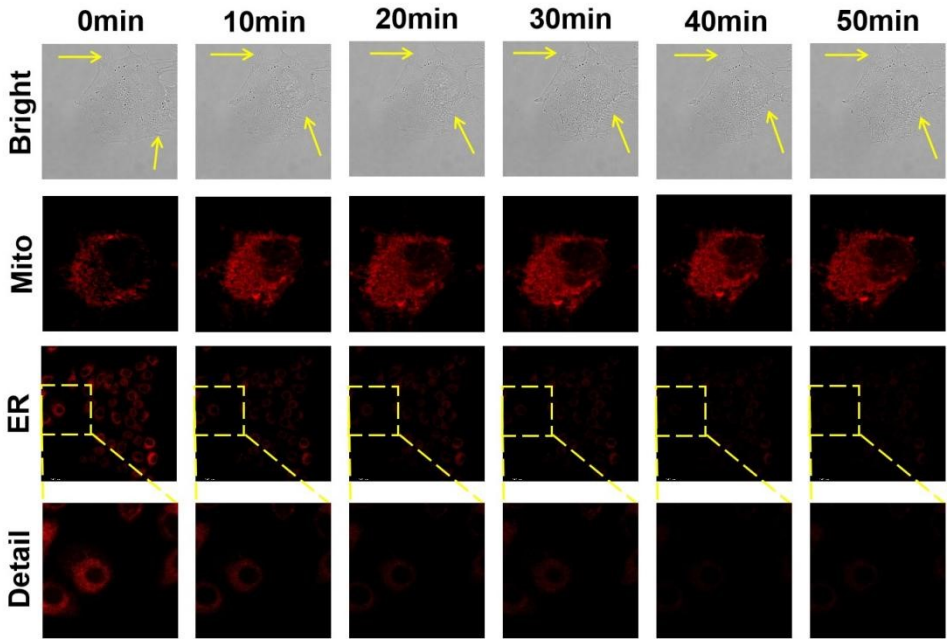


**Fig. S28** Changes in cell morphology, mitochondria and ER during cuproptosis after copper and DSF pre-treatment within 0-50 minutes.

The yellow arrows indicate the location of cell membrane rupture; the yellow boxes show magnified detail images of specific cells.

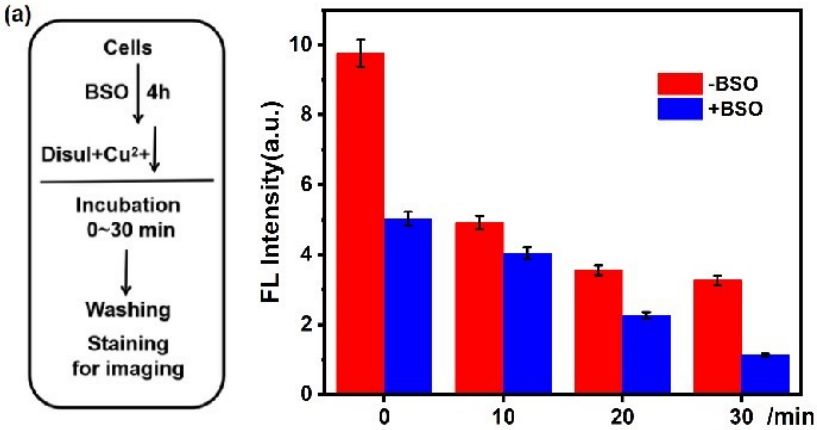


**Fig. S29** Effect of BSO addition on BHCO fluorescence.
(a) Operation flowchart using BSO processing. (b) Fluorescence intensity bar chart with or without BSO treatment time-dependent.

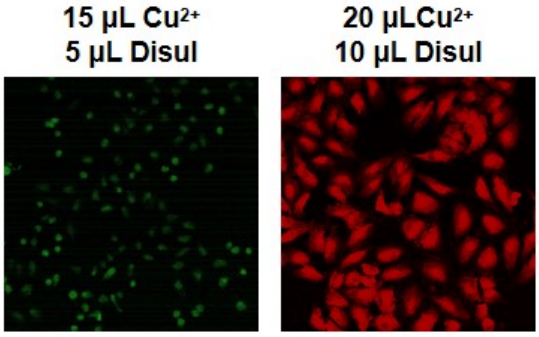


**Fig. S30** AM-PI was used for cell viability experiments after adding different concentrations of $Cu^{2+}$ and DSF.
(Red fluorescence represents dead cells; green fluorescence represents live cells).

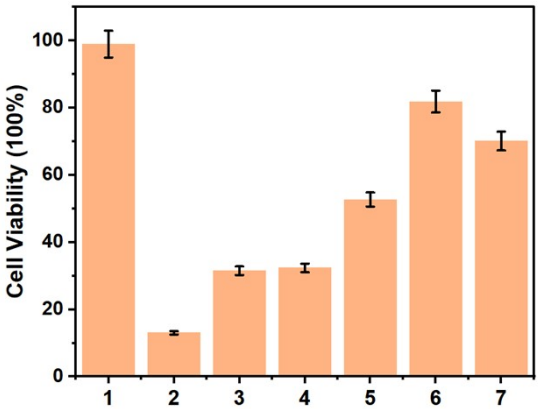


**Fig. S31** MTT method was used to measure the cell survival rate after treatment.
Add different inhibitors during BHCO induced cell death. 1: control; 2: BHCO+ $Cu^{2+}$+ DSF; 3: 2+ Fer-1; 4: 2+ NAC; 5: 2+ TTM; 6: 2+ Fer-1+ TTM; 7: 2+ NAC+ TTM.

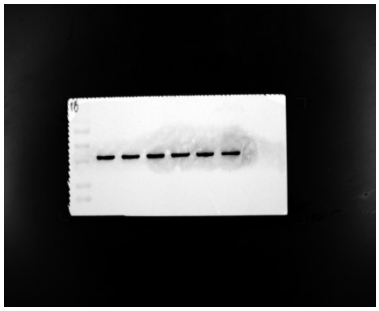

(A) β-actin

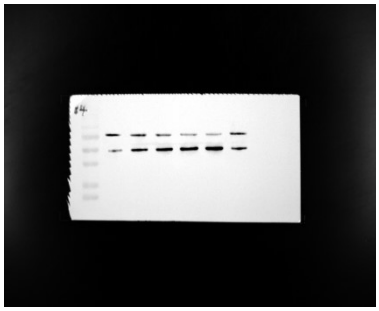

(B) DLAT

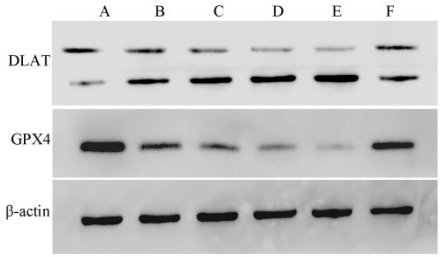


(C)

**Fig. S32** Western blot analysis of the DLAT expressions of HeLa cells incubated under different treatments. A: Control group; B-E: BHCO + 0, 20, 40, 60 μL $Cu^{2+}$ + DSF; F: BHCO + $Cu^{2+}$ (60 μL) + DSF + TTM (60 μL)

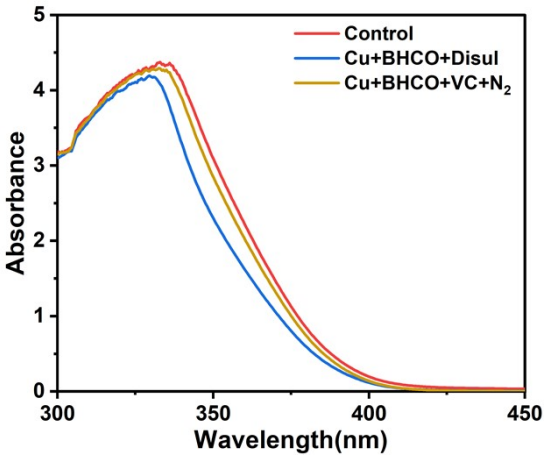


**Fig. S33** Measurement of intracellular GSH content.

1: Control group, 2: adding BHCO and DSF-Cu, 3: adding cuproptosis inhibitors on the basis of 2; 4: adding ferroptosis inhibitors on the basis of 2.

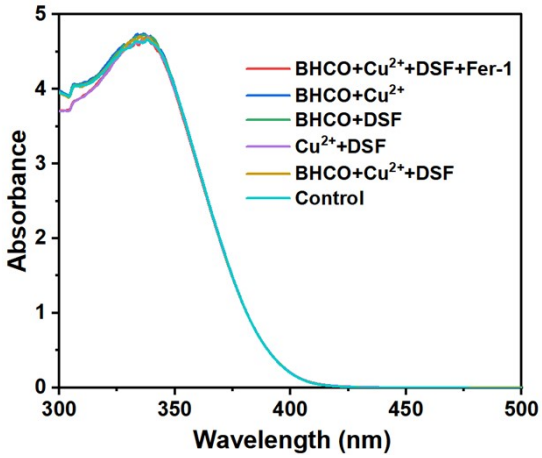


**Fig. S34** Measurement of intracellular GSH content.

0: Control, 1: BHCO+ DSF, 2: BHCO+ $Cu^{2+}$, 3: $Cu^{2+}$+ DSF, 4: BHCO+ DSF+ $Cu^{2+}$, 5: BHCO+ DSF+ $Cu^{2+}$+ Fer-1.

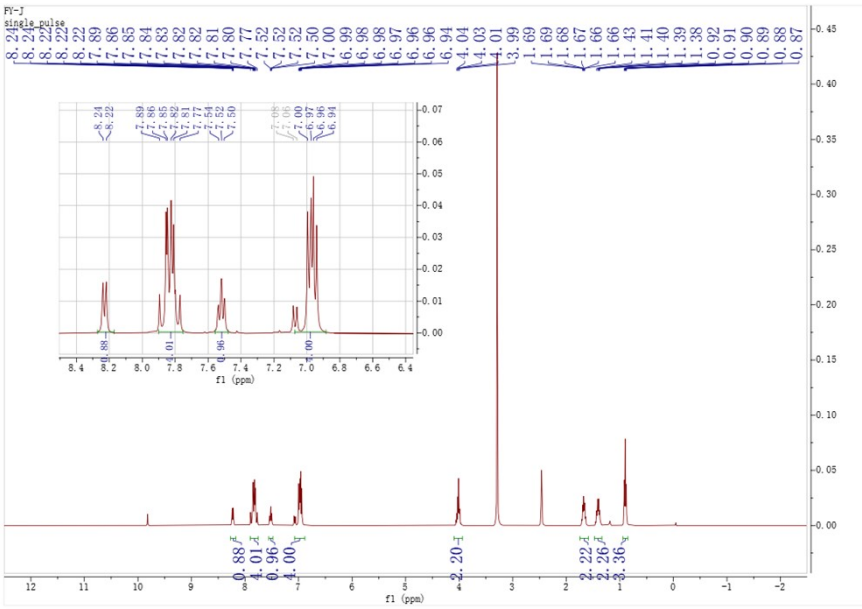

**Fig. S35** $^{1}$H NMR spectrum of BHEO.

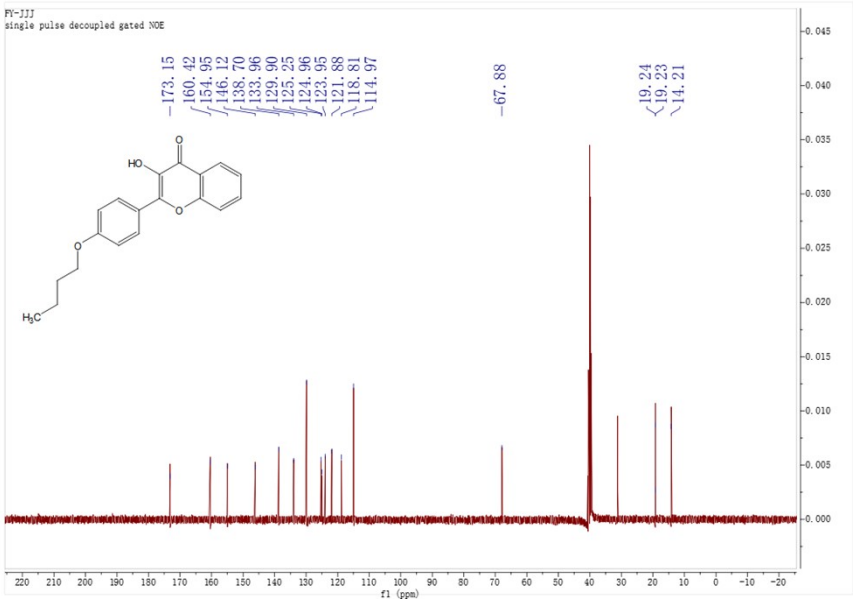


**Fig. S36** $^{13}$C NMR spectrum of BHCO.

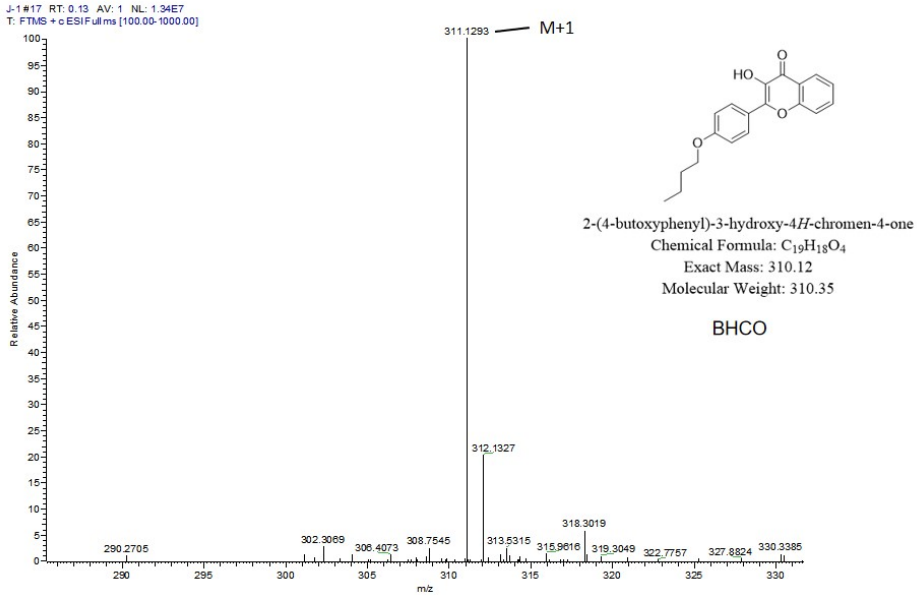


**Fig. S37** Mass spectrum of BHCO.

| Intensity | δ | K/541 nm | K/427 nm | LOD/μM /541 nm | LOD/μM /427 nm |
|---|---|---|---|---|---|
| 8613 | | 4855.2857 | 3266.857 | 0.00537807 | 0.007993024 |
| 8622 | | 385.7 | 246.8 | 0.067700457 | 0.105802537 |
| 8630 | 8.704022059 | | | | |
| 8634 | | | | | |
| 8637 | | | | | |

**Table 1** Calculation of detection limits of BHCO under 427 nm and 541 nm.